MOLECULAR IMAGING AND BIOLOGY

Mol Imaging Biol (2014) 16:412–420
DOI: 10.1007/s11307-013-0711-2

Published Online: 5 December 2013

World Molecular Imaging Society

RESEARCH ARTICLE

Imaging Tumour ATB$^{0,+}$ Transport Activity by PET with the Cationic Amino Acid *O*-2((2-[^{18}F]fluoroethyl)methyl-amino)ethyltyrosine

Adrienne Müller,[1] Aristeidis Chiotellis,[1] Claudia Keller,[1] Simon M. Ametamey,[1] Roger Schibli,[1,2,3] Linjing Mu,[2] Stefanie D. Krämer[1]

[1]*Center for Radiopharmaceutical Sciences ETH-PSI-USZ, Institute of Pharmaceutical Sciences, ETH Zurich, Wolfgang-Pauli-Strasse 10, 8093, Zurich, Switzerland*

[2]*Center for Radiopharmaceutical Sciences ETH-PSI-USZ, Department of Nuclear Medicine, University Hospital Zurich, Zurich, Switzerland*

[3]*Center for Radiopharmaceutical Sciences ETH-PSI-USZ, Paul Scherrer Institute, Villigen, Switzerland*

Abstract

Purpose: The concentrative amino acid transporter ATB$^{0,+}$ (SLC6A14) is under evaluation as a target for anticancer therapy. An ATB$^{0,+}$-selective positron emission tomography (PET) probe could advance preclinical drug development. We characterised the cationic tyrosine analogue *O*-2((2-[^{18}F]fluoroethyl)methyl-amino)ethyltyrosine ([^{18}F]FEMAET) as a PET probe for ATB$^{0,+}$ activity.

Procedures: Cell uptake was studied *in vitro*. ATB$^{0,+}$ expression was quantified by real-time PCR. [^{18}F]FEMAET accumulation in xenografts was investigated by small animal PET with mice.

Results: [^{18}F]FEMAET accumulated in PC-3 and NCI-H69 cancer cells *in vitro*. As expected for ATB$^{0,+}$ transport, uptake was inhibited by LAT/ATB$^{0,+}$ inhibitors and dibasic amino acids, and [^{18}F]FEMAET efflux was only moderately stimulated by extracellular amino acids. ATB$^{0,+}$ was expressed in PC-3 and NCI-H69 but not MDA-MB-231 xenografts. PET revealed accumulation in PC-3 and NCI-H69 xenografts and significant reduction by ATB$^{0,+}$ inhibition. Uptake was negligible in MDA-MB-231 xenografts.

Conclusion: ATB$^{0,+}$ activity can be imaged *in vivo* by PET with [^{18}F]FEMAET.

Key words: ATB$^{0,+}$, SLC6A14, Positron emission tomography, PET, Tyrosine, Cationic amino acid, PC-3, NCI-H69, MDA-MB-231, FEMAET

Introduction

Cancer cells have augmented nutrient transport and metabolism to cope with their enhanced activities in cell proliferation and survival [1]. Upregulated nutrient transporters and metabolising enzymes provide potential targets for anticancer therapy and diagnosis. For instance, expression of glucose transporters GLUT (solute carrier SLC2A subfamily) and hexokinases is increased in most types of cancer. Both are targets of the glucose analogue 2-deoxy-2-[^{18}F]fluoro-D-glucose ([^{18}F]FDG), the most frequently applied probe for tumour imaging by positron emission tomography (PET) [2].

Among the amino acid transporters, LAT1 and LAT3 (SLC7A5 and SLC43A1), ASCT2 (SLC1A5), xCT

Correspondence to: Stefanie D. Krämer; *e-mail:* stefanie.kraemer@pharma.ethz.ch

(SLC7A11), and ATB$^{0,+}$ (SLC4A16) are upregulated in many cancer types [1, 3]. Figure 1 shows an overview of their transport characteristics. The amino acid PET probes 6-[^{18}F]fluoro-L-DOPA ([^{18}F]FDOPA), *O*-(2-[^{18}F]fluoroethyl)-L-tyrosine ([^{18}F]FET) and 5-(2-[^{18}F]fluoroethoxy)-L-tryptophan ([^{18}F]FEHTP) accumulate in tumour cells *via* LAT1, an obligatory exchange system for large neutral amino acids [1, 4–6]. Besides LAT, also ASCT2 and xCT are exchange transporters. The ASCT2 substrate [^{18}F]fluciclovine (anti-[^{18}F]FACBC), a leucine derivative which is currently under clinical investigation, shows promising characteristics for the imaging of aggressive prostate cancer [7, 8]. Among these transporters, only ATB$^{0,+}$ is unidirectional. It has the unique property to transport its substrates even against a concentration gradient from extra- to intracellular. While LAT, ASCT2 and xCT promote influx of neutral amino acids, ATB$^{0,+}$ recognises also cationic besides neutral amino acids [1].

ATB$^{0,+}$ overexpression has so far been shown in breast, colorectal and cervical cancers and cell lines of colon and breast cancer [1, 9]. Compared to other amino acid transport systems, it has relatively low expression levels in healthy tissue. Significant expression was detected in lung, trachea, salivary glands, mammary glands and pituitary gland and lower levels in colon, uterus, prostate and testis [10, 11]. ATB$^{0,+}$ is characterised by a broad substrate specificity, including D-amino acids. The unidirectional concentrative transport is driven by transmembrane gradients of sodium and chloride ions and more generally by the membrane potential [1, 12]. The transporter is currently under investigation as a drug target for cancer therapy. Inhibition of ATB$^{0,+}$ with α-methyl-DL-tryptophan (αMTRP), a LAT and ATB$^{0,+}$ inhibitor, resulted in reduction of xenograft size in nude mice *in vivo* and autophagy of tumour cells *in vitro* [9, 13]. Besides direct inhibition for anticancer therapy, the transporter may be targeted to deliver cytotoxic drugs into tumour cells. Hatanaka *et al.* have shown transport by ATB$^{0,+}$ of side chain esterified aspartate (β-carboxyl group) and glutamate (γ-carboxyl group) [11]. Esterification at the α-carboxyl group or at the side chain hydroxyl group of amino acids could offer alternative approaches for drug or pro-drug delivery into tumour cells *via* ATB$^{0,+}$ transport [11, 12].

ATB$^{0,+}$ may thus become a target for multiple approaches in anticancer therapy. Since not every cancer type has elevated ATB$^{0,+}$ levels [9], enhanced ATB$^{0,+}$ activity by the primary tumour or metastases needs to be confirmed before an ATB$^{0,+}$-targeting therapy is started. Molecular/functional imaging allows non-invasive quantification of regional expression levels or activities of target proteins. An ATB$^{0,+}$-selective PET probe may help evaluating ATB$^{0,+}$-targeting drug candidates *in vivo* in preclinical drug development programs. It may in addition serve in the future to recognise ATB$^{0,+}$-positive tumours to identify patients who could benefit from anticancer therapy with an ATB$^{0,+}$-targeting drug or pro-drug.

In this work, we evaluated our recently introduced cationic amino acid PET probe *O*-2((2-[^{18}F]fluoroethyl)methylamino)ethyltyrosine ([^{18}F]FEMAET, Fig. 2) [14] as a substrate and selective PET probe for ATB$^{0,+}$. We studied the characteristics of transport into and out of ATB$^{0,+}$-expressing PC-3 prostate cancer and NCI-H69 small cell lung cancer cells *in vitro* and chose three cancer models according to their ATB$^{0,+}$ mRNA levels as determined by real-time PCR for *in vivo* PET studies, namely PC-3 and NCI-H69 as ATB$^{0,+}$-positive and

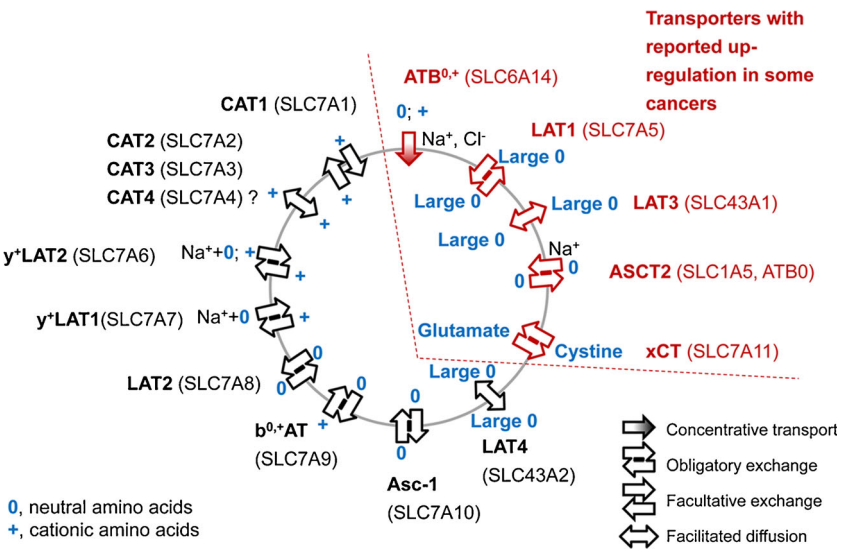

Fig. 1. Schematic overview of amino acid transporters. Symbols are explained in the figure. Na^++0 indicates Na^+-cotransport with a neutral amino acid. ATB$^{0,+}$ transport is dependent on Na^+/Cl^- gradients/membrane potential. ASCT2 transport is Na^+ dependent. ATB$^{0,+}$, LAT1, LAT3, ASCT2 and xCT can be upregulated in cancer cells (references see text). Cell polarisation is not considered in the figure.

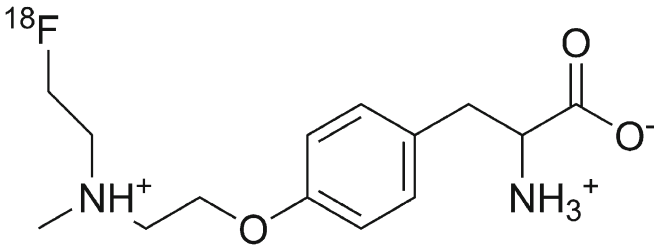

Fig. 2. Structure of [18F]FEMAET.

breast cancer MDA-MB-231 as $ATB^{0,+}$-negative tumours. These three tumour models accumulated the LAT1 substrate [18F]FEHTP under identical experimental conditions [6]. Finally, we investigated the effect of the $ATB^{0,+}$ inhibitor αMTRP on [18F]FEMAET accumulation in NCI-H69 xenografts *in vivo* to address the potential of [18F]FEMAET PET to evaluate $ATB^{0,+}$-modifying agents *in vivo*.

Materials and Methods

Radiosynthesis of [18F]FEMAET and In Vitro Cell Studies

[18F]FEMAET was produced by nucleophilic substitution of a fully tert-butyl protected chloride precursor, synthesised from L-tyrosine, with non-carrier-added [18F]KF-$K_{2.2.2}$ complex in DMSO and subsequent deprotection as described elsewhere [14]. Specific radioactivity was between 28 and 45 GBq/μmol at a radiochemical purity of >99 %. The stereochemistry of the final product was not investigated. For *in vitro* and *in vivo* experiments, [18F]FEMAET was formulated in phosphate-buffered saline (PBS) containing 10 mg/ml sodium ascorbate (pH 7–8) and 5 % ethanol.

PC-3 and NCI-H69 cells were purchased from the German Collection of Microorganisms and Cell Cultures, Cell Lines Service (DSMZ, Braunschweig, Germany) and were cultured according to the supplier's protocols. Twenty-four hours before a transport assay, PC-3 cells were seeded at 13,000 cells/cm^2 in 48-well plates (Costar; Corning) and NCI-H69 cells were subcultured in suspension into fresh medium. One hour before the assay, cells were washed and incubated at 37 °C with 400 μL Earle's balanced salt solution (1 mio NCI-H69 cells per tube) containing Ca^{2+} and Mg^{2+} (EBSS, Invitrogen) [6].

For uptake studies, 20 kBq [18F]FEMAET was added to each well or tube (time zero), and cells were incubated at the indicated temperature on a shaker at 25 rpm (PC-3) or 130 rpm (NCI-H69) and washed twice with ice cold incubation solution at the indicated time points. PC-3 cells were detached with 0.25 % trypsin/1 mM EDTA (Invitrogen); NCI-H69 cells were pelleted by centrifugation and radioactivity was quantified in a gamma counter and decay-corrected (Perkin Elmer Wizard 1480). Protein content of the lysed cells (2 % sodium dodecyl sulphate) was quantified in parallel with the DC Protein Assay (Bio-Rad) and bovine serum albumin as standard. For inhibition experiments, 10 mM (final concentration) 2-amino-2-norboranecarboxylic acid (BCH), 10 mM L-arginine, 10 mM L-lysine, 10 mM L-histidine (PC-3) or 1 mM αMTRP (NCI-H69) were added in 20 μL 100 mM phosphate buffer (all pH between 7.0 and 8.0) immediately before addition of the radiotracer.

For [18F]FEMAET efflux experiments, PC-3 cells were incubated with tracer as described above for 60 min and washed twice with ice cold EBSS before 400 μl EBSS containing 800 μM L-leucine, 10 mM L-lysine or the respective volume of EBSS (all pH between 7.0 and 8.0) was added (time zero). The plates were incubated at 37 °C, and cells were washed twice with the respective ice cold incubation solution at the indicated time points, detached and analysed as described above.

Expression Levels of $ATB^{0,+}$ in Cultured Cells and Xenografts

Total RNA was isolated from PC-3, NCI-H69 and MDA-MB-231 (American Type Culture Collection) cell lines and the respective xenografts according to the protocols of the Isol-RNA Lysis Reagent (5 PRIME) and the bead-milling TissueLyser system (Qiagen). QuantiTect® Reverse Transcription Kit (Qiagen) was used to generate cDNA. The following primers (Microsynth) were used for the polymerase chain reaction (PCR): human beta-actin (ACTB), forward 5′-CATGTACGTTGCTATCCAGGC-3′, reverse 5′-CTCCTTAATGTCACGCACGAT-3′ and human $ATB^{0,+}$ (SLC6A14), forward 5′-TGGGGTCCATACCTGGAACA-3′, reverse 5′-TGCTGCCACTAACAGTAGGT-3′. Quantitation of $ATB^{0,+}$ expression was performed with the DyNAmoTM Flash SYBR® Green qPCR Kit (Thermo Scientific) using a 7900 HT Fast Real-Time PCR System (Applied Biosystems). The amplification signals were detected in real-time, which permitted accurate quantification of the amounts of the initial RNA template during 40 cycles according to the manufacturer's protocol. All reactions were performed in duplicates and within three independent runs. Quantitative analysis was performed using the SDS Software (v2.4) and a previously described $2^{-\Delta\Delta Ct}$ quantification method [15]. The specificity of the PCR products of each run was determined and verified with the SDS dissociation curve analysis feature.

PET with Xenograft-Bearing Mice

Animal care and experiments were conducted in compliance with Swiss Animal Welfare legislation and have been approved by the Veterinary Office of the Canton Zurich, Switzerland. Six weeks old female NMRI nu/nu mice from Charles River, Sulzfeld (Germany) were inoculated with 2×10^6 PC-3 cells in 0.1 ml PBS/matrigel 1:1 (Invitrogen; BP Biosciences) or 2×10^6 MDA-MB-231 cells in 0.1 ml matrigel subcutaneously on the right shoulder. For NCI-H69 xenografts, mice were inoculated with 10^7 NCI-H69 cells in 0.1 ml PBS subcutaneously on the right shoulder and 1 week later with the same cell number in matrigel on the left shoulder. Xenografts were grown for several weeks until they reached 0.5 to 1.5 cm^3. Mice had free access to food and water. For dynamic scans from 1 to 90 min post injection (p.i.), one mouse with a PC-3 and one with an MDA-MB-231 xenograft were injected under anaesthesia (2–3 % isoflurane in oxygen/air) with 13 and 15 MBq [18F]FEMAET, respectively, in 0.1 ml formulation into a tail vein and a dynamic PET scan (Vista eXplore, Sedecal, Spain, axial field of view 4.8 cm) was started about 1 min later. For dynamic scans from 60 to 150 min (one mouse each with a PC-3 and MDA-MB-231 xenograft) and static scans from 60 to 90 min (six NCI-H69 xenograft-bearing mice for the inhibition study with αMTRP), mice were injected awake in a restraining tube with 5.6 to 14 MBq

[18F]FEMAET as described above. Anaesthesia was induced 10 min before PET acquisition. In static scans, anterior and posterior body parts were scanned for 15 min each, starting with the anterior part. In the inhibition study, NCI-H69 xenograft-bearing mice were injected 100 mg/kg αMTRP in 100 mM phosphate buffer pH 7.4 (5 mg αMTRP per ml) intraperitoneally 15 min before intravenous [18F]FEMAET injection. Control animals were injected the same volume vehicle only. During all scans, respiratory rate and body temperature were monitored and controlled between 50 and 70 beats per minute and 36 and 37 °C by adjusting the isoflurane dose and with 37 °C warm air, respectively. The PET scans were followed by a CT for anatomical orientation. PET data was reconstructed by 2-dimensional ordered subsets expectation maximisation and analysed with PMOD 3.4 (PMOD, Zürich, Switzerland). Volumes of interest (VOI) were delineated with help of the CT and PET images and standardised uptake values (SUV) were calculated for the VOIs as the ratio of regional averaged radioactivity in becquerel per cubic centimetre and injected radioactivity in becquerel per gram body weight. Radioactivity was decay-corrected for all calculations. SUV ratios in the inhibition study with αMTRP were compared by a two-tailed homoscedastic *t* test.

Results

Cell Uptake and Efflux Studies

As a cationic amino acid, [18F]FEMAET may be transported by the exchange transporters CATs, y^+LAT2 and $b^{0,+}$AT or the concentrative transporter $ATB^{0,+}$ but not by LAT1/2 (Fig. 1) [16]. We have recently shown uptake of [18F]FEMAET into NCI-H69 small cell lung cancer cells *in vitro* and *in vivo* and suspected transport by $ATB^{0,+}$ as the primary uptake mechanism [14]. In this work, we investigated the mechanism of cell uptake of [18F]FEMAET in more detail. To verify transport by $ATB^{0,+}$, we studied the effect of αMTRP, an inhibitor of $ATB^{0,+}$ (and LAT1) on [18F]FEMAET uptake in NCI-H69 cells. As shown in Fig. 3a, 1 mM αMTRP inhibited uptake by >65 % at 37 °C and to ~30 % at 4 °C after 30 min incubation, the time point when uptake at 37 °C approached a plateau under identical experimental conditions [14].

Figure 3b shows [18F]FEMAET accumulation in prostate cancer PC-3 cells at 37 °C, reaching 8.8±1.6 % uptake per mg protein at 60 min (n=10). Uptake at 4 °C was significantly lower with 1.9±1.0 %/mg. Figure 3c shows the effects of the (LAT1/2 and) $ATB^{0,+}$ inhibitor BCH [10, 16, 17] and natural amino acids with basic side chains on [18F]FEMAET uptake into PC-3 cells. BCH reduced [18F]FEMAET uptake by more than 90 %. The cationic dibasic amino acids L-arginine and L-lysine, influx substrates of CATs, y^+LAT2, $b^{0,+}$AT and $ATB^{0,+}$ [10, 13, 17] as well as the neutral dibasic L-histidine, influx substrate at physiological pH of LATs [18] and $ATB^{0,+}$ [10, 13] reduced [18F]FEMAET uptake, though to a lower extent than BCH.

Extracellular stimulation of an exchange transporter accelerates efflux of its substrates [16]. Figure 3d shows depletion within 5 min of the LAT substrate [18F]FDOPA from PC-3 cells after addition of 800 μM L-leucine. A similar rapid depletion was observed for the LAT substrate [18F]FEHTP [6]. We expected that a selective $ATB^{0,+}$ substrate would not be recognised by exchange transporters. Extracellular amino acids should, therefore, not accelerate its efflux as tremendously as observed for the LAT1/2 substrates. As shown in Fig. 3e, f, both 800 μM of the LAT substrate L-leucine and 10 mM of the cationic amino acid L-lysine had only moderate effects on the efflux of [18F]FEMAET from PC-3 cells as compared to its efflux in the absence of stimulation. At 30 min after stimulation, radioactivity in cells was >50 % of the control without stimulation. Based on the above results, we hypothesised that transport by $ATB^{0,+}$ is the primary mechanism for [18F]FEMAET uptake.

Expression of $ATB^{0,+}$ in NCI-H69, PC-3 and MDA-MB-231 Cells and Xenografts

As mentioned in the "Introduction", not all cancers overexpress $ATB^{0,+}$. We confirmed expression of the transporter in both PC-3 and NCI-H69 cell lines by real-time PCR (Fig. 4). As shown by Karunakaran *et al.* [9], we did not find significant expression of $ATB^{0,+}$ in MDA-MB-231 breast cancer cells. Based on our real-time PCR analysis and cell uptake experiments, we proceeded with *in vivo* PET studies with PC-3, NCI-H69 and MDA-MB-231 xenograft-bearing mice, expecting uptake of [18F]FEMAET into PC-3 besides NCI-H69 [14] xenografts but negligible uptake into the $ATB^{0,+}$-negative MDA-MB-231 xenografts. In agreement with the analysis of the cultured cells, $ATB^{0,+}$ was significantly expressed in PC-3 and NCI-H69 but not in MDA-MB-231 xenografts, as determined by real-time PCR (Fig. 4).

PET Studies with Mice Bearing $ATB^{0,+}$-Positive and $ATB^{0,+}$-Negative Xenografts and Inhibition of Uptake by αMTRP

Figure 5 shows PET images of PC-3 ($ATB^{0,+}$-positive) and MDA-MD-231 ($ATB^{0,+}$-negative) xenograft-bearing mice averaged from 60 to 90 min and from 120 to 150 min, respectively, after [18F]FEMAET administration. The corresponding time–activity curves (TACs) and radioactivity ratios between PC-3 xenografts and opposite shoulder are shown in Fig. 6. [18F]FEMAET accumulated in PC-3 xenografts. The SUV ratio between xenograft and opposite shoulder reached 2.5 towards the end of the 60–150 min scan. As expected, no or only negligible accumulation was observed in the $ATB^{0,+}$-negative MDA-MB-231 xenografts.

Finally, we investigated whether [18F]FEMAET uptake into $ATB^{0,+}$-positive NCI-H69 xenografts can be inhibited by an $ATB^{0,+}$ inhibitor. Application of 100 mg/kg αMTRP significantly reduced the SUV ratio between NCI-H69

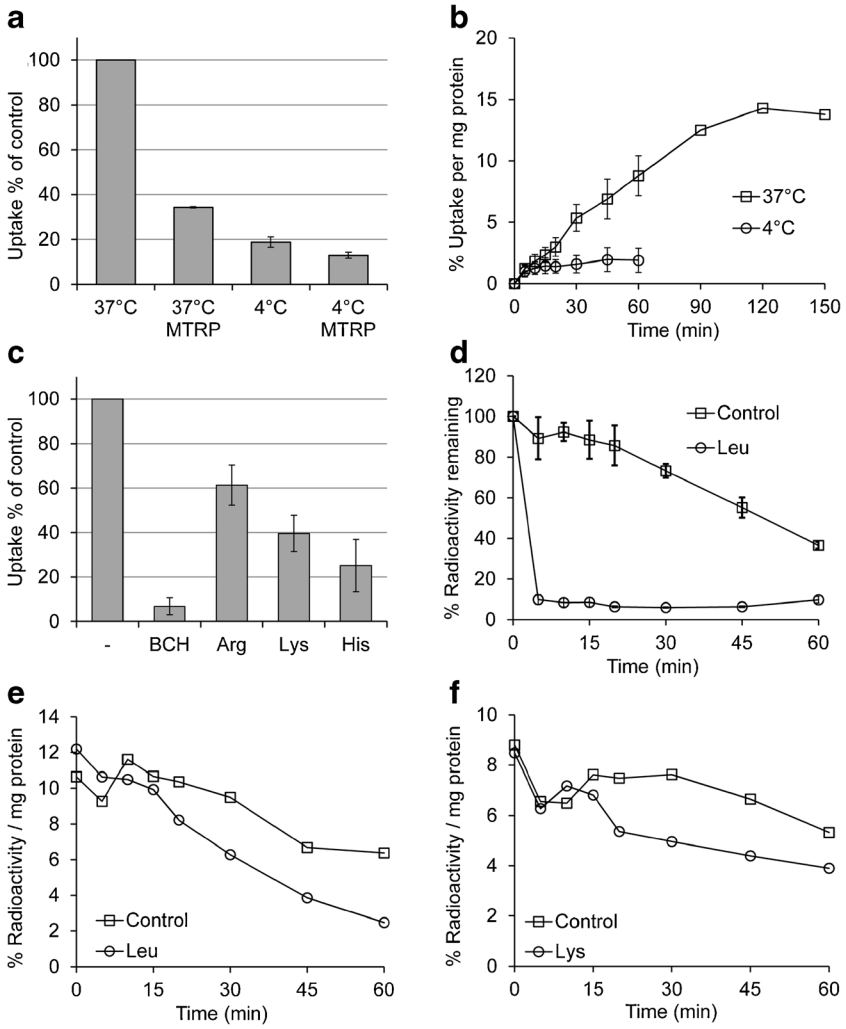

Fig. 3. **a** Uptake of [18F]FEMAET into NCI-H69 cells after 30 min at 37 and 4 °C and inhibition by 1 mM αMTRP (MTRP). Averages of two independent experiments each normalised to uptake %/mg protein at 37 °C. *Error bars* indicate values of the single experiments. The complete time course of [18F]FEMAET uptake in NCI-H69 cells without αMTRP is shown elsewhere [14]. **b** Uptake of [18F]FEMAET into PC-3 cells at 37 °C (*white square*) and 4 °C (*white circle*). **c** PC-3 cells were incubated with [18F]FEMAET for 60 min at 37 °C in the absence of other amino acids (-) or together with 10 mM BCH, L-arginine (*Arg*), L-lysine (*Lys*) or L-histidine (*His*). Uptake was normalised to %/mg without inhibitor. *Error bars* indicate standard deviations ($n \geq 3$). **d–f** PC-3 cells were incubated with [18F]FDOPA (**d**) or [18F]FEMAET (**e**, **f**) for 60 min at 37 °C before *trans*-stimulation. **d** Efflux of [18F]FDOPA after *trans*-stimulation with 800 μM L-leucine (*white circle*, $n=2$) or without *trans*-stimulation (control, *white square*, $n=3$) at 37 °C. *Error bars* indicate standard deviations (control) or the values of the single experiments (L-leucine). **e**, **f** Efflux of [18F]FEMAET with (*white circle*) and without (control, *white square*) *trans*-stimulation by 800 μM L-leucine (*Leu*) (**e**) and 10 mM L-lysine (*Lys*) (**f**), one experiment each. Most data in panel **d** were published before [6].

xenografts and neck region from 2.11±0.38 to 1.67±0.18 (averaged from 60 to 75 min p.i.; $n=5$ xenografts of three baseline mice and six xenografts of three blocked mice, respectively, $p<0.05$). Note that the PET image shown in [14] is from one of the baseline scans.

Discussion

We have recently introduced the cationic amino acid PET probe [18F]FEMAET and have shown uptake into NCI-H69 small cell lung cancer cells *in vitro* and xenografts in mice [14]. Transport systems that promote cell uptake of cationic amino acids are CATs, y^+LATs, $b^{0,+}$AT and $ATB^{0,+}$ (Fig. 1). Here, we provide strong evidence that [18F]FEMAET is selectively targeting the amino acid transporter $ATB^{0,+}$, which is upregulated in several cancer types and is under investigation as a drug target for anticancer therapy [9]. As concluded from the relatively low uptake ratios between xenografts and reference tissue, [18F]FEMAET will not compete with other amino acid tracers such as [18F]FET or anti-[18F]FACBC for tumour imaging in general. However, [18F]FEMAET allows to evaluate the expression and activity of $ATB^{0,+}$, a feature which could advance the development and support the clinical use of $ATB^{0,+}$-targeting drugs.

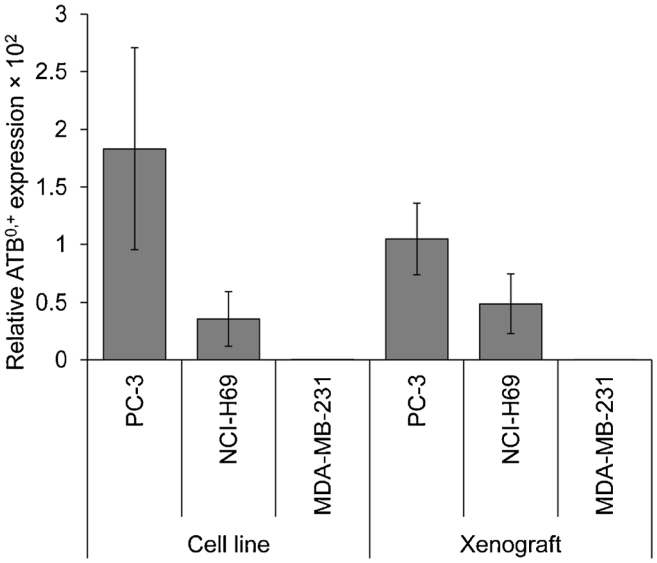

Fig. 4. Quantitative real-time PCR. $ATB^{0,+}$ expression levels were quantified relative to beta-actin in the indicated cancer cell lines and xenografts. Average ± standard error.

Evidence for selective $ATB^{0,+}$ targeting by [18F]FEMAET comes from *in vitro* cell experiments and *in vivo* PET studies. [18F]FEMAET uptake into PC-3 (this work) and NCI-H69 cells (this work and [14]) *in vitro* was significant at 37 °C but low at 4 °C, indicating that transport is energy dependent. This is expected for $ATB^{0,+}$ transport, which is driven by the membrane potential [1, 12]. BCH, a substrate and competitive inhibitor of LAT1/2 and $ATB^{0,+}$ reduced uptake into PC-3 cells *in vitro* by >90 %. Transport by LAT1 or LAT2 can be excluded based on the fact that [18F]FEMAET is cationic at physiological pH while LAT1 and LAT2 only recognise net neutral amino acids as substrates for transport [16]. The known competitive inhibitors of $ATB^{0,+}$, L-arginine, L-lysine and L-histidine [13], all reduced [18F]FEMAET uptake at 10 mM.

The efflux of the LAT1/2 substrates [18F]FDOPA and [18F]FEHTP [6] from PC-3 and NCI-H69 cells was strongly accelerated by the addition of the LAT1/2 substrate L-leucine to the cells. Only moderate acceleration of [18F]FEMAET efflux was observed after *trans*-stimulation with the same concentration of L-leucine and with L-lysine. L-Leucine activates efflux of neutral amino acids by LAT1/2 and cationic amino acids by y^+LAT1/2 [16, 19]. L-Lysine activates efflux of neutral amino acids by $b^{0,+}$AT and cationic amino acids by y^+LAT2 and CAT1 [16]. Based on the weak effect of *trans*-stimulation on [18F]FEMAET efflux, we conclude that none of these exchange transporters recognises [18F]FEMAET as a substrate neither for uptake nor for efflux.

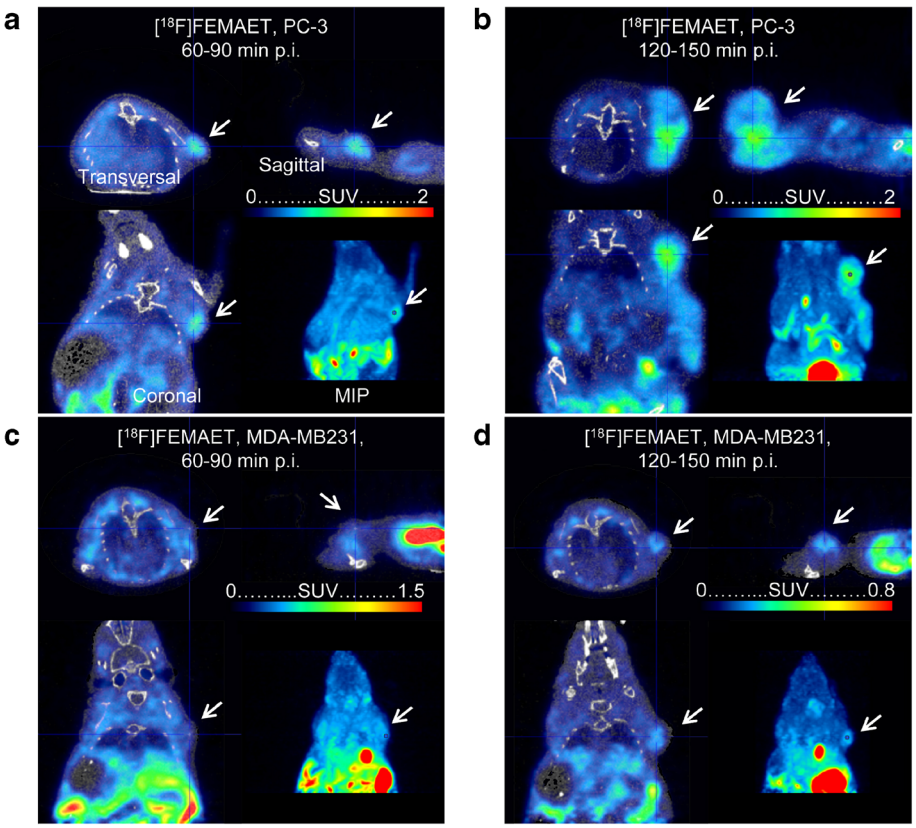

Fig. 5. PET/CT images of xenograft-bearing mice after [18F]FEMAET administration. **a**, **b** $ATB^{0,+}$-positive PC-3 xenografts; **c**, **d** $ATB^{0,+}$-negative MDA-MB-231 xenografts. **a**, **c** Averaged from 60 to 90 min p.i.; **b**, **d** averaged from 120 to 150 min p.i. *Arrows* indicate xenografts. *MIP* maximal intensity projection. Colour scale, PET SUV; *white*/*grey* CT. SUV scales were adjusted to result in similar colour (*blue*) for background tissue in all images.

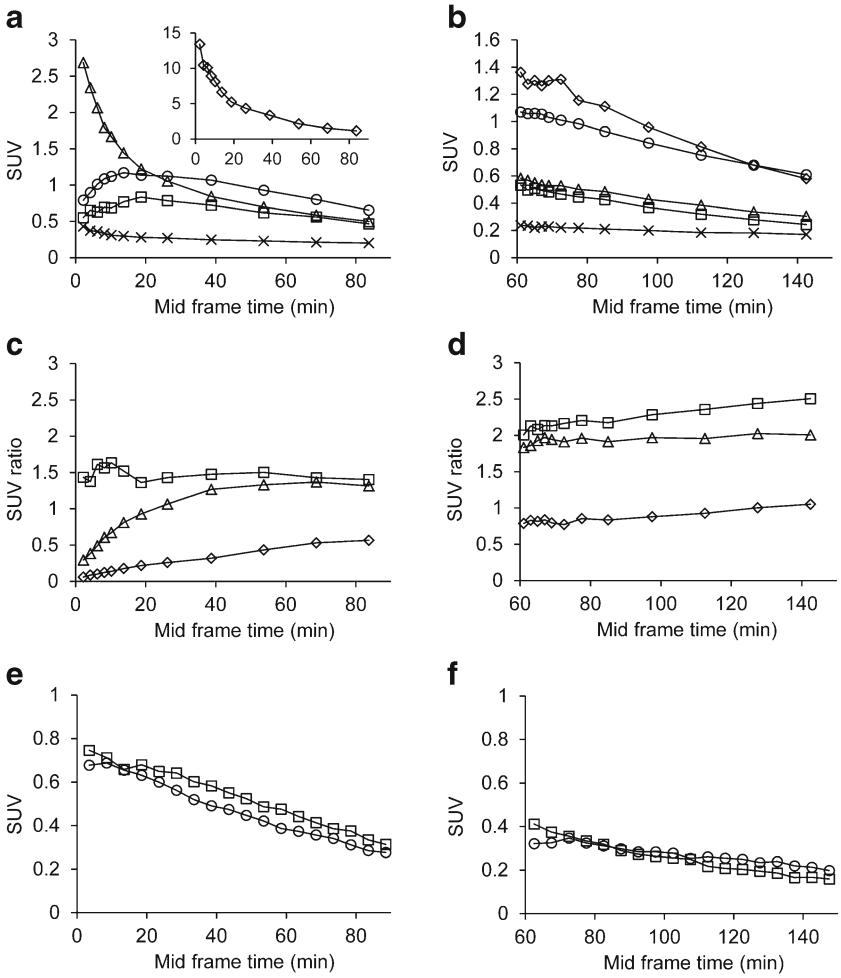

Fig. 6. TACs (**a**, **b**, **e**, **f**) and radioactivity ratios (**c**, **d**) from the [^{18}F]FEMAET PET scans shown in Fig. 5. **a**, **c**, **e** 0–90 min scans; **b**, **d**, **f** 60–150 min scans. **a**, **b** PC-3 mice, xenograft (*white circle*), opposite shoulder (*white square*), kidney (*white diamond* in insert), liver (*white triangle*), brain (*multiplication sign*). **c**, **d** Corresponding xenograft-to-tissue ratios (symbols of tissues as in **a**, **b**, **e**, **f**) TACs with MDA-MB-231 mice. Symbols as in **a** and **b**.

More evidence for ATB$^{0,+}$ transport comes from the uptake inhibition in NCI-H69 cells by 1 mM of the LAT and ATB$^{0,+}$ transport inhibitor αMTRP by up to 66 %. For comparison, Karunakaran *et al.* found 80 % inhibition of glycine transport at the same αMTRP concentration in ATB$^{0,+}$-transfected oocytes [13]. IC_{50} was estimated to 0.25 mM [13]. Note that the transporter is thus not fully saturated at 1 mM αMTRP. Besides the *in vitro* experiments, the PET studies strongly supported our hypothesis that [^{18}F]FEMAET accumulates in cancer cells by ATB$^{0,+}$ transport. First, the ATB$^{0,+}$ inhibitor αMTRP reduced tumour uptake of [^{18}F]FEMAET. Assuming homogenous distribution of the inhibitor in body water, the 100 mg/kg dose resulted in a maximal concentration of ≤0.7 mM, decreasing with time. No complete transport inhibition can be expected at this dose, considering the IC_{50} of 0.25 mM. Nevertheless, we found significant reduction in tumour/reference tissue ratio after αMTRP application. Second, [^{18}F]FEMAET did not accumulate in the ATB$^{0,+}$-negative MDA-MB-231 xenografts. Finally, in contrast to LAT1 substrates, [^{18}F]FEMAET was excluded from the brain after intravenous administration in mouse [14]. This would be expected for a substrate of ATB$^{0,+}$ such as [^{18}F]FEMAET, as ATB$^{0,+}$ is absent in the brain [10] and as amino acids, in general, require a transport system to cross the blood–brain barrier. Altogether, our data strongly supports our hypothesis that ATB$^{0,+}$ transport is the major mechanism of [^{18}F]FEMAET uptake into cancer cells *in vitro* and *in vivo*. Further studies with transporter expression systems and/or targeted silencing of transporters with, *e.g.* siRNA will reveal the extent of contribution of alternative transport systems to [^{18}F]FEMAET cell uptake.

We assign selectivity for ATB$^{0,+}$ transport to the following structure characteristics: (a) The tertiary amine of the amino acid side chain renders [^{18}F]FEMAET cationic at physiological pH with an expected pK_a between 10 and 11 [20]. This impedes recognition by transport systems for neutral amino acids such as LAT. (b) ATB$^{0,+}$ has a less

restrictive recognition pattern than the other amino acid transport systems. The non-natural amino acid structure of [18F]FEMAET may exclude recognition by other transporters than ATB0,+. (c) The metabolic stability of [18F]FEMAET *in vivo* and in human microsomes excludes accumulation *via* a biotransformation step [14]. We modified tyrosine by ether coupling to the 5-hydroxy group rather than by an ester or amide bond at a carboxyl group as suggested for pro-drug design [11]. In contrast to pro-drugs, hydrolysis of the PET probe was not desired.

We are not aware of any other basic and cationic amino acid that is currently in use or under investigation for PET imaging. A promising new amino acid PET probe with a basic side chain, the triazole (*S*)-2-amino-3-[1-(2-[18F]fluoroethyl)-1*H*-[1–3]triazol-4-yl]propanoic acid ([18F]AFETP), was recently introduced by the group of McConathy [21, 22]. In contrast to [18F]FEMAET, the side chain with the substituted 1*H*-[1–3]-triazole is only weakly basic and is most probably neutral at physiological pH [20, 23, 24]. Cell uptake of [18F]AFETP was reduced by the same natural amino acids as we found for [18F]FEMAET but in contrast to [18F]FEMAET only to 31 % by the ATB0,+ and LAT1/2 inhibitor BCH. The authors concluded that [18F]AFETP must be recognised by more than one amino acid transport system [22].

Expression of ATB0,+ is upregulated in oestrogen-sensitive breast cancer, in carcinoma of the cervix and colorectal cancer [9, 25, 26]. In addition, several oestrogen receptor positive cancer cell lines express ATB0,+ [9, 13]. This is not surprising as the *SLC6A14* (ATB0,+) promoter contains several putative binding domains for the oestrogen receptors [9]. PC-3 cells as many other prostate cancer cells have high expression levels of the oestrogen receptors [27]. ATB0,+ upregulation is, therefore, likely in these and other prostate cancer cells. We have confirmed its expression in the PC-3 cell line. Interestingly, we also found high expression in NCI-H69 cells which lack oestrogen, progesterone and androsterone receptors and have only low levels of glucocorticoid receptor [28]. This indicates that a high level of oestrogen receptor is not a prerequisite for ATB0,+ overexpression. Besides oestrogen receptor-mediated induction, protein kinase C increases ATB0,+ activity in cancer cells [29].

ATB0,+ expression levels in most healthy tissues are relatively low [9, 25, 26]. This together with its concentrative transport mechanism and its broad substrate specificity makes ATB0,+ a good target for anticancer therapy [9, 13] and drug and pro-drug delivery [12]. ATB0,+ could thus become of interest as a target for non-invasive imaging to advance the development of ATB0,+-targeting drugs and in the context of tumour characterisation for therapy planning and therapy monitoring. Regarding drug development, [18F]FEMAET PET could help evaluating the *in vivo* potency of ATB0,+ inhibitors as well as the transport efficiency of ATB0/+-targeting drugs and pro-drugs.

We used L-tyrosine for [18F]FEMAET synthesis but did not confirm the stereochemistry of the final product [14]. In general, ATB0,+ recognises both L- and D-amino acids [12]. However, we cannot exclude that transport kinetics differ significantly between the two isomers. We have recently discussed the influence of stereochemistry on PET imaging with amino acid derivatives in more detail [30]. Further evaluation, including synthesis and confirmation of stereochemically pure enantiomers is required to address this question for [18F]FEMAET.

Conclusions

The cationic amino acid PET probe [18F]FEMAET is most probably selectively targeting ATB0,+, a concentrative amino acid transporter that is under preclinical evaluation for anticancer therapy and as a target for drug and pro-drug delivery. As [18F]FEMAET uptake into xenografts is reduced by ATB0,+ inhibition, the probe may serve to characterise potential ATB0,+ inhibitors and substrates for anticancer therapy. In the long range, [18F]FEMAET PET may be used to identify patients that could benefit from ATB0,+-targeted anticancer therapy and to monitor therapy effects.

Acknowledgments. We thank Romana Meletta for the technical help with the RNA isolation and cDNA preparation.

Conflict of Interest. The authors declare that they have no conflict of interest.

References

1. Ganapathy V, Thangaraju M, Prasad PD (2009) Nutrient transporters in cancer: relevance to Warburg hypothesis and beyond. Pharmacol Ther 121:29–40
2. Jadvar H, Alavi A, Gambhir SS (2009) 18F-FDG uptake in lung, breast, and colon cancers: molecular biology correlates and disease characterization. J Nucl Med 50:1820–1827
3. Bodoy S, Fotiadis D, Stoeger C *et al* (2012) The small SLC43 family: facilitator system L amino acid transporters and the orphan EEG1. Mol Aspects Med 34:638–645
4. Neels OC, Koopmans KP, Jager PL *et al* (2008) Manipulation of [11C]-5-hydroxytryptophan and 6-[18F]fluoro-3,4-dihydroxy-L-phenylalanine accumulation in neuroendocrine tumor cells. Cancer Res 68:7183–7190
5. Langen KJ, Hamacher K, Weckesser M *et al* (2006) O-(2-[18F]fluoroethyl)-L-tyrosine: uptake mechanisms and clinical applications. Nucl Med Biol 33:287–294
6. Krämer SD, Mu L, Müller A *et al* (2012) 5-(2-18F-fluoroethoxy)-L-tryptophan as a substrate of system L transport for tumor imaging by PET. J Nucl Med 53:434–442
7. Sorensen J, Owenius R, Lax M, Johansson S (2013) Regional distribution and kinetics of [18F]fluciclovine (anti-[18F]FACBC), a tracer of amino acid transport, in subjects with primary prostate cancer. Eur J Nucl Med Mol Imaging 40:394–402
8. Okudaira H, Nakanishi T, Oka S *et al* (2013) Kinetic analyses of trans-1-amino-3-[18F]fluorocyclobutanecarboxylic acid transport in *Xenopus laevis* oocytes expressing human ASCT2 and SNAT2. Nucl Med Biol 40:670–675
9. Karunakaran S, Ramachandran S, Coothankandaswamy V *et al* (2011) SLC6A14 (ATB0,+) protein, a highly concentrative and broad specific amino acid transporter, is a novel and effective drug target for treatment of estrogen receptor-positive breast cancer. J Biol Chem 286:31830–31838

10. Sloan JL, Mager S (1999) Cloning and functional expression of a human Na^+- and Cl^--dependent neutral and cationic amino acid transporter B0+. J Biol Chem 274:23740–23745
11. Hatanaka T, Haramura M, Fei YJ *et al* (2004) Transport of amino acid-based prodrugs by the Na^+- and Cl^--coupled amino acid transporter ATB0,+ and expression of the transporter in tissues amenable for drug delivery. J Pharmacol Exp Ther 308:1138–1147
12. Ganapathy ME, Ganapathy V (2005) Amino acid transporter ATB$^{0,+}$ as a delivery system for drugs and prodrugs. Curr Drug Targets Immune Endocr Metabol Disord 5:357–364
13. Karunakaran S, Umapathy NS, Thangaraju M *et al* (2008) Interaction of tryptophan derivatives with SLC6A14 (ATB$^{0,+}$) reveals the potential of the transporter as a drug target for cancer chemotherapy. Biochem J 414:343–355
14. Chiotellis A, Müller A, Weyermann K, *et al*. (2013) Synthesis and preliminary biological evaluation of O-2((2-[^{18}F]fluoroethyl)methylamino)ethyltyrosine ([^{18}F]FEMAET) as a possible cationic amino acid PET tracer for tumor imaging (submitted)
15. Livak KJ, Schmittgen TD (2001) Analysis of relative gene expression data using real-time quantitative PCR and the 2(-Delta Delta C(T)) Method. Methods 25:402–408
16. Verrey F, Closs EI, Wagner CA *et al* (2004) CATs and HATs: the SLC7 family of amino acid transporters. Pflug Arch Eur J Physiol 447:532–542
17. Deves R, Boyd CA (1998) Transporters for cationic amino acids in animal cells: discovery, structure, and function. Physiol Rev 78:487–545
18. Kanai Y, Segawa H, Miyamoto K *et al* (1998) Expression cloning and characterization of a transporter for large neutral amino acids activated by the heavy chain of 4F2 antigen (CD98). J Biol Chem 273:23629–23632
19. Kanai Y, Fukasawa Y, Cha SH *et al* (2000) Transport properties of a system y^+L neutral and basic amino acid transporter. Insights into the mechanisms of substrate recognition. J Biol Chem 275:20787–20793
20. Comer JEA (2007) Ionization constants and ionization profiles. In: Van de Waterbeemd H, Testa B (eds) Comprehensive medicinal chemistry II. Elsevier, Oxford, pp 357–397
21. McConathy J, Zhou D, Shockley SE *et al* (2010) Click synthesis and biologic evaluation of (*R*)- and (*S*)-2-amino-3-[1-(2-[^{18}F]fluoroethyl)-1*H*-[1,2,3]triazol-4-yl]propanoic acid for brain tumor imaging with positron emission tomography. Mol Imaging 9:329–342
22. Sai KKS, Huang C, Yuan L *et al* (2013) ^{18}F-AFETP, ^{18}F-FET, and ^{18}F-FDG imaging of mouse DBT gliomas. J Nucl Med 54:1120–1126
23. Ryazanova OA, Voloshin IM, Makitruk VL *et al* (2007) pH-induced changes in electronic absorption and fluorescence spectra of phenazine derivatives. Spectrochim Acta A Mol Biomol Spectrosc 66:849–859
24. Tomé AC (2004) Product class 13: 1,2,3-triazoles. In: Stor R, Gilchrist T (eds) Science of synthesis, vol 13. Georg Thieme, Stuttgart, pp 415–601
25. Gupta N, Miyauchi S, Martindale RG *et al* (2005) Upregulation of the amino acid transporter ATB$^{0,+}$ (SLC6A14) in colorectal cancer and metastasis in humans. Biochim Biophys Acta 1741:215–223
26. Gupta N, Prasad PD, Ghamande S *et al* (2006) Up-regulation of the amino acid transporter ATB$^{0,+}$ (SLC6A14) in carcinoma of the cervix. Gynecol Oncol 100:8–13
27. Pandini G, Genua M, Frasca F *et al* (2007) 17beta-estradiol up-regulates the insulin-like growth factor receptor through a nongenotropic pathway in prostate cancer cells. Cancer Res 67:8932–8941
28. Kaiser U, Hofmann J, Schilli M *et al* (1996) Steroid-hormone receptors in cell lines and tumor biopsies of human lung cancer. Int J Cancer 67:357–364
29. Samluk L, Czeredys M, Skowronek K, Nalecz KA (2012) Protein kinase C regulates amino acid transporter ATB$^{0,+}$. Biochem Biophys Res Commun 422:64–69
30. Chiotellis A, Mu L, Müller A *et al* (2013) Synthesis and biological evaluation of ^{18}F-labeled fluoropropyl tryptophan analogues as potential PET probes for tumor imaging. Eur J Med Chem 70C:768–780